CHEMMEDCHEM

DOI: 10.1002/cmdc.200800212

β′-Hydroxy-α,β-unsaturated ketones: A new pharmacophore for the design of anticancer drugs. Part 2.**

Leticia G. León,[a, b] Rubén M. Carballo,[a] María C. Vega-Hernández,[a, c] Pedro O. Miranda,[a] Víctor S. Martín,[a] Juan I. Padrón,[a, d] and José M. Padrón*[a, b]

Novel antiproliferative β′-acyloxy-α,β-unsaturated ketones were obtained by means of an iron(III)-catalyzed multicomponent domino process (ABB′ 3CR). The most active derivatives displayed GI_{50} values in the range of 0.5–3.9 μM against a panel of representative human solid tumor cell lines: A2780, SW1573, HBL-100, T-47D and WiDr. Analysis of cells following 24 h exposure to these drugs showed cell cycle arrest in the S and G_2/M phase, in a dose-dependent manner. Our data indicate that the β′-acyloxy-α,β-unsaturated ketones cause permanent damage to the cells and induce apoptosis.

Introduction

Natural products remain the most important source of inspiration for medicinal chemists in the development of new anticancer drugs. These privileged structures, with their inherent drug-likeness, have proven to be an extremely powerful tool to aid the discovery of potent and selective antitumor drugs for a wide variety of cellular targets.[1] Phytochemicals have provided an abundant source of novel therapeutics for the treatment of human cancers. In this particular context, natural dietary agents including fruits, vegetables, and spices have shown their ability to suppress cancers.[2]

Avocado has received considerable attention due to its chemopreventive properties. Although epidemiological studies have shown the health benefits of avocado, the cellular and molecular mechanisms of the phytochemicals responsible for cancer prevention are largely unknown.[3] Avocados contain a number of phytochemicals, however, we have focused our attention on the so-called "aliphatic acetogenins". Aliphatic acetogenins are long aliphatic hydrocarbon chains (C_{16} to C_{21}) with varying degrees of saturation, and three oxygenated functional groups (1,2,4-trihydroxy or 1,2-dihydroxy-4-oxo). The former have shown moderate cytotoxicity against cancer cell lines[4] whilst the latter appear to be promising cancer chemopreventive agents.[5] It was reported earlier that the absolute configuration of the secondary hydroxyl group in this type of products is not a critical factor for biological activity.[5] Figure 1 shows representative examples of the natural products found in avocado, including the long chain 1,2-dihydroxy-4-oxo alkanols persenone A (**1**), persenone B (**2**), persin (**3**) and isopersin (**4**).

Persenones A (**1**) and B (**2**) have a common β′-hydroxy-α,β-unsaturated ketone framework. Recently, we reported the synthesis of a library of α,β-unsaturated ketones, and their cytotoxic activity against both sensitive and resistant human solid tumor cell lines.[6] The β′-hydroxy-α,β-unsaturated ketone moiety was established as the pharmacophore with the substituents modulating the biological activity. An additional advantage of the synthetic derivatives is their fast, simple, and versatile synthesis. Thus, β′-hydroxy-α,β-unsaturated ketones can be synthesized in a single step using a modular and diversity-oriented method.[7] This multicomponent domino process is promoted by inexpensive and environmentally friendly iron(III). Multicomponent reactions[8] have attracted the attention of synthetic and medicinal chemists, as they constitute efficient tools for the modular and diversity-oriented construction of molecular complexity.

In this study, we report the synthesis and cytotoxic activity of selected derivatives of β′-acyloxy-α,β-unsaturated ketones against a panel of representative human solid tumor cells: A2780 (ovarian), SW1573 (non-small cell lung), HBL-100 (breast), T-47D (breast) and WiDr (colon). Growth inhibition parameters were determined using the NCI protocol with slight modifications.[9] For the most active compounds, cell cycle and apoptosis studies were performed to deduce their possible mechanism.

[a] *Dr. L. G. León, R. M. Carballo, Dr. M. C. Vega-Hernández, Dr. P. O. Miranda, Prof. V. S. Martín, Dr. J. I. Padrón, Dr. J. M. Padrón*
Instituto Universitario de Bio-Orgánica "Antonio González" (IUBO-AG)
Universidad de la Laguna
C/ Astrofísico Francisco Sánchez, 2, 38206 La Laguna (Spain)
Fax: (+34) 922-318-571
E-mail: jmpadron@ull.es

[b] *Dr. L. G. León, Dr. J. M. Padrón*
BioLab, Instituto Canario de Investigación del Cáncer (ICIC)
C/ Astrofísico Francisco Sánchez, 2, 38206 La Laguna (Spain)

[c] *Dr. M. C. Vega-Hernández*
Unidad de Investigación
Hospital Universitario de Canarias (HUC), Universidad de La Laguna
Campus de Ofra, 38320 La Laguna (Spain)

[d] *Dr. J. I. Padrón*
Instituto de Productos Naturales y Agrobiología
Consejo Superior de Investigaciones Científicas (CSIC)
C/ Astrofísico Francisco Sánchez 3, 38206 La Laguna (Spain)

[**] *Part 1: see reference [6]*

Supporting information for this article is available on the WWW under http://dx.doi.org/10.1002/cmdc.200800212.

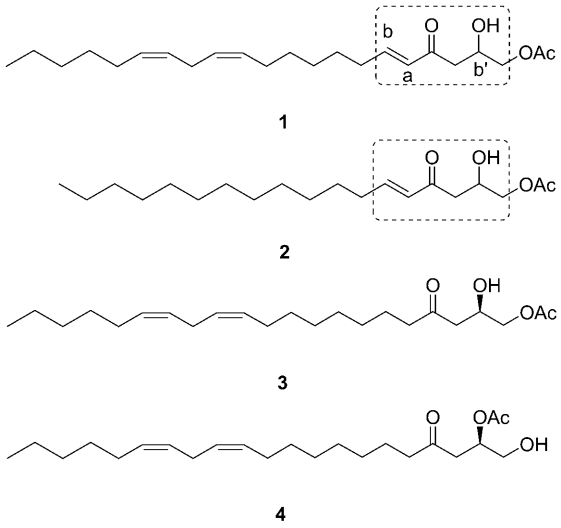

Figure 1. Naturally occurring 1,2-dihydroxy-4-oxo alkanols found in avocado.

Results and Discussion

Synthesis of α-Branched α,β-unsaturated ketones

The reaction of aldehydes and olefins under iron(III) catalysis is a versatile process that leads to a wide variety of derivatives.[10] In this particular context, we have focused our attention on the coupling of an aliphatic aldehyde **5** and a propargylic alcohol **6**, in which the alkyne group is internal. The catalytic system is compatible with unprotected alcohols and their corresponding acetates (Scheme 1). This single step strategy allows the synthesis of α-branched α,β-unsaturated ketones **8a**–**b**. A proposed mechanism for this reaction is shown in Figure 2. The Lewis acid FeX_3 activates aldehyde **5**, which condenses with the propargylic derivative **6**. This adduct converts to the cyclic intermediate **7**, which after a rearrangement gives compound **8**.

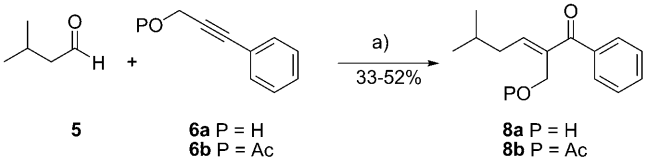

Scheme 1. Synthesis of α-branched α,β-unsaturated ketones: a) $FeCl_3$, CH_2Cl_2, RT, 1 min.

Synthesis of linear β′-hydroxy α,β-unsaturated ketone derivatives

Our approach to the synthesis of the β′-hydroxy-α,β-unsaturated ketone pharmacophore is based on a three-component reaction (3CR) between homopropargylic alcohols and aldehydes. The β′-hydroxy-α,β-unsaturated ketone fragment arises from the chemo-differentiated incorporation of two aldehyde units and one homopropargylic alcohol unit. The proposed mechanism for this ABB′ 3CR[11] is outlined in Figure 3. Two

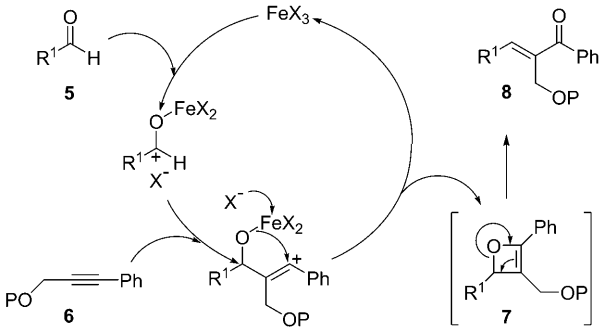

Figure 2. The proposed mechanism for the synthesis of compound **8**.

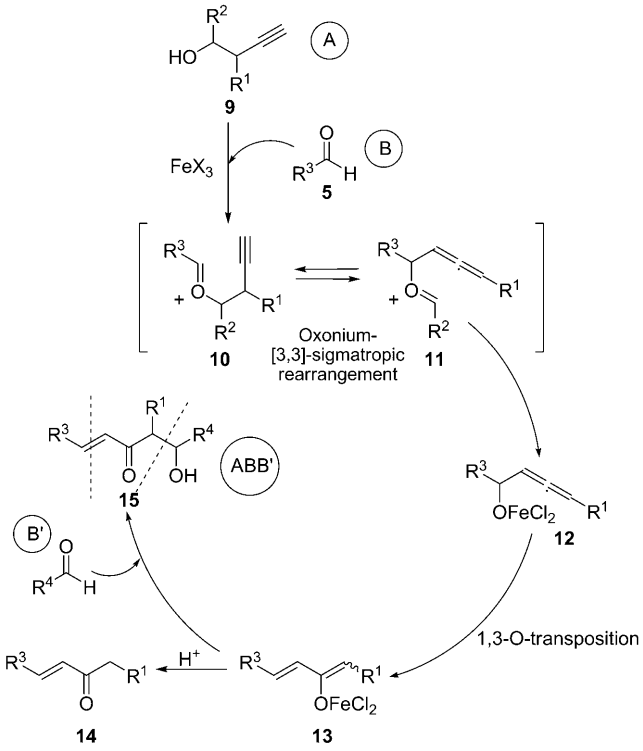

Figure 3. Iron(III) catalyzed ABB′ 3CR domino process.

important consequences can be seen from the mechanism. Firstly, the method allows preparation of cross-over products when two different aldehydes are being reacted ($R^3 \neq R^4$). Secondly, this synthetic strategy does not tolerate homopropargylic acetates, and therefore the acetylated derivative of compound **15** cannot be synthesized in a one-pot reaction. We applied this versatile synthetic methodology to prepare the set of β′-hydroxy-α,β-unsaturated ketone derivatives and evaluated their antiproliferative activity.[6]

Antiproliferative activity

The in vitro antiproliferative activity of all compounds was assessed in A2780, SW1573, HBL-100, T-47D and WiDr human solid tumor cells, and the results are shown in Table 1. The GI_{50}

Table 1. Lipophilicity and GI_{50} values of selected derivatives against human solid tumor cells.[a]

Compound	Clog P[b]	A2780 (ovarian)	SW1573 (lung)	HBL-100 (breast)	T-47D (breast)	WiDr (colon)
8a	3.09	18 (±2.5)	24 (±3.3)	n.t.	38 (±5.3)	19 (±8.7)
8b	4.21	2.1 (±0.4)	1.8 (±1.4)	n.t.	25 (±0.2)	3.5 (±2.1)
16a	5.52	26 (±2.0)	25 (±4.2)	n.t.	>100	31 (±6.2)
16b	6.42	13 (±3.8)	23 (±2.4)	n.t.	18 (±2.6)	18 (±2.4)
17a	4.48	2.1 (±1.0)	3.8 (±1.3)	2.3 (±0.3)	17 (±6.7)	2.9 (±1.5)
17b	5.37	0.5 (±0.2)	2.2 (±0.5)	1.8 (±0.7)	2.0 (±0.9)	3.9 (±1.6)
17c	7.07	1.2 (±0.5)	3.2 (±1.4)	1.6 (±0.8)	1.7 (±0.8)	3.1 (±0.2)

[a] Values are given in μM and are means of at least three experiments; standard deviation is given in parentheses. [b] Ref. [14].

values[12] for branched α,β-unsaturated ketones show that the acetylated derivative **8b** is 9 times more potent than the alcohol **8a** in the ovarian cell line A2780, and 5 and 12 times more potent in the drug-resistant cell lines SW1573 and WiDr, respectively. However, in T-47D cells the difference is smaller (1.5-times). This observation, together with the presence of acetyl groups in naturally occurring alkanols (**1**-**4**), encouraged us to study the effect of hydroxyl protection on linear β′-hydroxy-α,β-unsaturated ketones. In a preliminary cytotoxicity screen,[6] compounds **16a** was as potent, and derivative **17a** was more potent than the branched analogue **8a**. Derivatives **16a** and **17a** were selected as representative examples of linear β′-hydroxy-α,β-unsaturated ketones, and the corresponding acetates **16b** and **17b** were prepared by standard methods (Scheme 2). In addition to the acetates, derivative **17c**, which bears a benzoyl group, a more bulky group than the acyl group, was prepared.

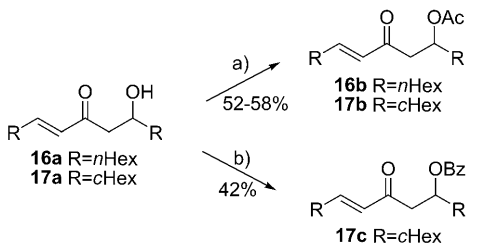

Scheme 2. Synthesis of novel β′-hydroxy-α,β-unsaturated ketone derivatives. a) Ac_2O, py, RT, o/n; b) BzCl, py, RT, o/n.

The biological activity of the acylated compounds **16b** and **17b** revealed a similar trend; the acetates were more potent than the free hydroxy parent compounds (Table 1). The effect is most evident in the drug-resistant breast cancer cell line T-47D. Compound **16a** was inactive (GI_{50} >100 μM) against T-47D, whilst the analogous acetyl compound **16b** shows a GI_{50} value of 18 μM. Similarly, the acetate **17b** was nine times more potent against T-47D cells than the free hydroxy derivative **17a**. The benzoate **17c** was more potent than the parent compound **17a**, and displayed a similar activity profile to the corresponding acetate **17b**. Compound **17b** was the most potent derivative of the series with GI_{50} values in the range of 0.5–3.9 μM against all cell lines.

Lipophilicity

Lipophilicity is associated with drug solubility and drug permeability through cell membranes.[13] For this reason, lipophilicity is an important physicochemical property to take into account in the design and development of a drug. The octanol/water partition coefficient expressed in a logarithmic form (Clog P) is widely used for calculating drug lipophilicity. It is usually calculated from the sum of partition coefficients of the chemical fragments composing the molecule. Clog P[14] values for all tested compounds are given in Table 1, and are in the range 3–7. Overall, lipophilicity is not sufficient to explain the observed differences in terms of antiproliferative activity.

Stability test

The modest yields obtained for the acylation of the linear β′-hydroxy α,β-unsaturated ketones **16a** and **17a** raised concern about the stability of the products. In particular, these acetates might be prone to elimination. To determine whether the acetate derivatives were stable under the conditions used in the biological experiments, we designed and performed a drug stability test. The UV spectrum of a phosphate buffer saline (PBS) solution (pH 7.4) of compound **17a** or **17b** (200 μM), was recorded at different time intervals. No substantial changes were observed in the UV spectra, indicating that the compounds were stable under the experimental conditions.

Cell cycle assay

Cell cycle control is the major regulatory mechanism of cell growth.[15] Many cytotoxic agents and/or DNA damaging agents arrest the cell cycle at the G_0/G_1, S, or G_2/M phase, and then induce apoptotic cell death. We examined cell cycle phase distribution by flow cytometry to determine whether cell growth inhibition involved cell cycle changes. The effect on the cell cycle was assessed in the five human solid tumor cell lines after 24 h exposure to the most active compounds **17a**–**c**. Cells were exposed to each agent at two different drug concentrations (high and low), which were chosen based on two premises:[16] The GI_{50} values of compounds **17a**–**c**, and the sensitivity of the cell line to drug treatment, since at higher drug doses cell death prevents examination of the cell cycle phase distribution. The most sensitive cells (A2780) were exposed to 5 (low) and 10 μM (high), and the SW1573 and HBL-100 cells were treated with 10 (low) and 20 μM (high). Finally, the drug-resistant cell lines T-47D and WiDr were treated with 20 (low) and 30 μM (low) of derivatives **17a**–**c**. Control cells were incubated in the absence of test drug.

The results of cell cycle distributions of samples collected from control and treated cells are summarized in Figure 4. In all cell lines, compounds **17a–c** induced cell cycle arrest in the

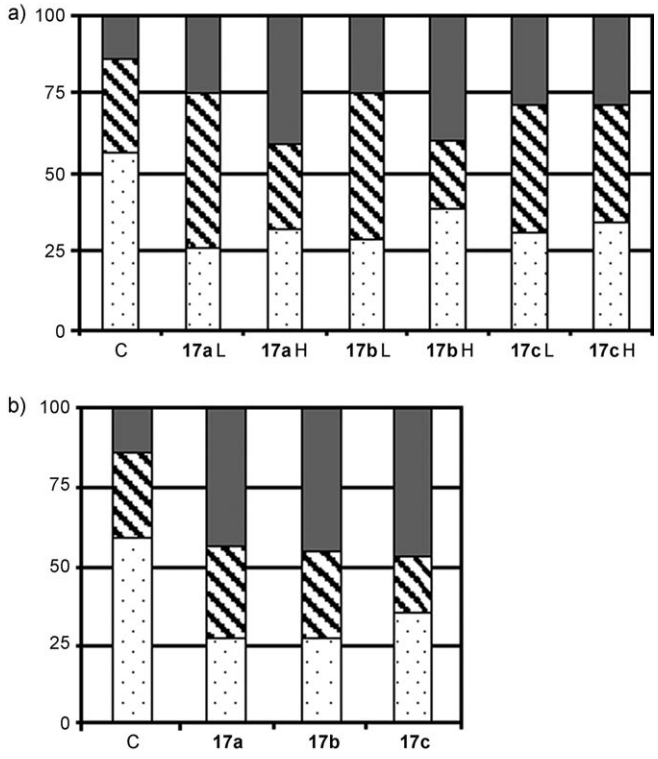

Figure 4. Cell cycle phase distribution in T-47D cells. a) untreated T-47D cells (C) and T-47D cells treated with compounds **17a-c** for 24 h at low (L) and high (H) dose concentrations; b) cells treated with the 24+24 drug schedule. Values represent means of at least two experiments. Dotted area = G_0/G_1, lined area = S, filled area = G_2/M.

S or G_2/M phases, in a dose dependent manner. The increase in S or G_2/M phase is concomitant with a decrease in the G_0/G_1 compartment. Remarkable results were obtained for the resistant T-47D cells (Figure 4). When the breast cancer cells were treated at a low drug concentration (20 μM) a similar level of arrest in both the S and G_2/M phases was observed for derivatives **17a–c**. However, at 30 μM (the high drug dose) only accumulation in the G_2/M phase was observed for compounds **17a–b** (Figure 5). Concomitant with this increase in the percentage of cells in the G_2/M phase was a parallel decrease in the percentage of cells in the G_0/G_1 phase. Compound **17c** showed no differences at the low and high drug doses.

These results suggest that derivatives **17a–c** inhibit proliferation of the selected cell lines via S and/or G_2/M phase arrest of the cell cycle. Differences have been observed between compounds **17a–b** and derivative **17c** in A2780 and T-47D cells. These differences cannot be explained in terms of GI_{50} values. Similar to analogues **17a–b**, cell cycle arrest in the G_2/M phase has been observed in T-47D cells treated with the natural product persin (**3**).[17]

The α,β-unsaturated ketone fragment is a Michael acceptor that can interact with nucleophiles inside the cell. Consequently, permanent damage to cells is likely to occur. Thus, we ex-

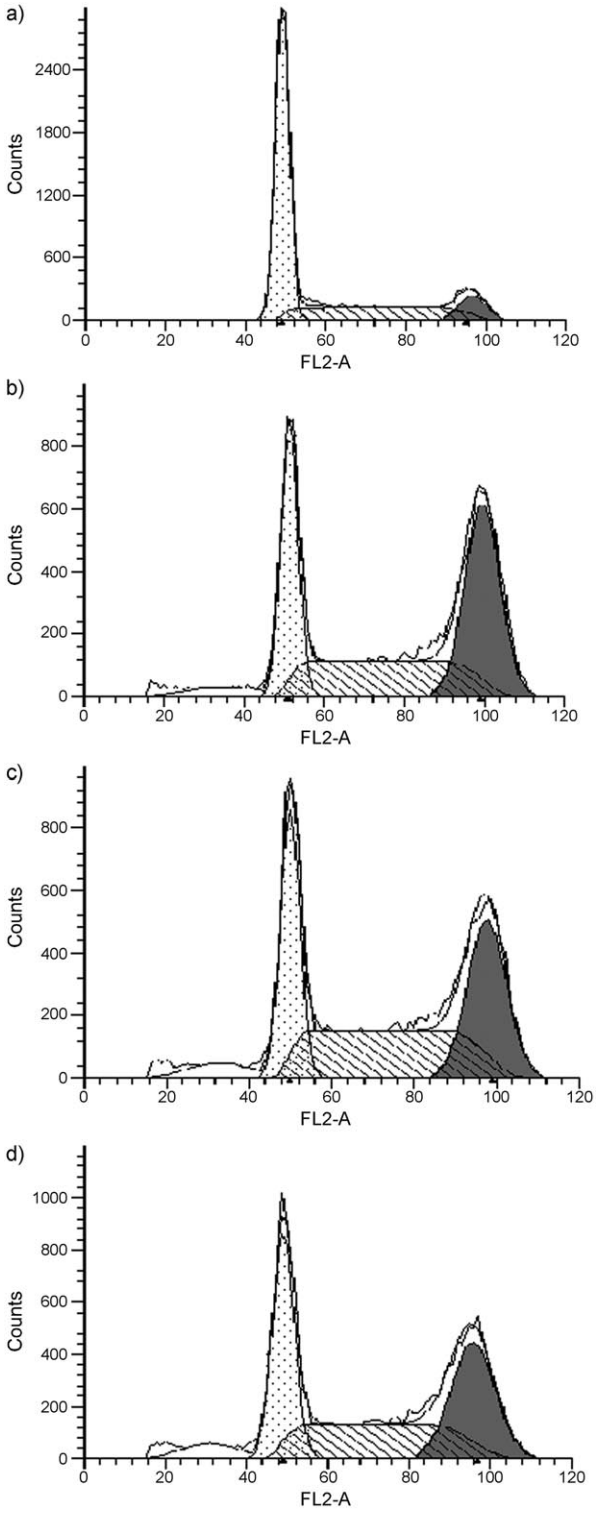

Figure 5. Histogram of T-47D cells after exposure to analogues **17a–c** (30 μM for 24 h). a) control; b) compound **17a**; c) compound **17b**; d) compound **17c**. Dotted area = G_0/G_1, lined area = S, filled area = G_2/M.

posed cells to drugs **17a–c** for a 24 h period, after which time the drug was washed away and cells were kept in a drug free medium for an additional period of 24 h, the so-called 24+24 drug schedule. Cells were then collected and their cell cycle distribution was examined. The drug doses chosen for these

experiments were 10 μM (A2780), 20 μM (SW1573, HBL-100 and WiDr) and 30 μM (T-47D).

Overall, compounds **17a–c** induced cell cycle arrest in all cell lines, which was persistent after the drug was washed away and cells had a 24 h period to recover. With the exception of A2780 cells, the percentage of cells in the S and G_2/M phase represent more than 60% of the cell population. The results indicate that the compounds permanently damage the cells, causing an accumulation of cells in the S and G_2/M phases prior to cell death. No clear difference was observed between the effects of the drugs **17a–c**.

Interestingly, in the breast cancer cell lines (HBL-100 and T-47D) the G_2/M compartment was larger after the overall treatment (Figure 4b) when compared to 24 h drug exposure (Figure 4a). However, this effect was not observed for the lung and colon cancer cell lines. Our findings in the breast cancer cell lines seem parallel to those that define persin (**3**) as a potential cancer therapeutic agent against breast cancer.[17,18]

Annexin V binding

Apoptosis or programmed cell death is a highly regulated form of cell death involving multiple signaling pathways. It is an energy-requiring process that is triggered when a cell has been damaged and cannot recover.[19] At the onset of apoptosis, the phosphatidyl choline residues of the cell membrane are translocated from the inner to the outer membrane surface. Annexin V-FITC is a fluorescent marker for the detection of phosphatidyl choline residues in cell membranes by flow cytometry. In combination with propidium iodide (PI), the method allows discrimination between viable cells (Annexin V−/PI−), cells in early apoptosis (Annexin V+/PI−), cells in late apoptosis (Annexin V+/PI+) and necrotic cells (Annexin V−/PI+).

Exposure of the cell lines to compounds **17a–c** for 24 h did not give a sufficient amount of apoptotic cells for analysis. From the cell cycle studies, we found that the sub-G_0 peak in the histograms was most evident with the 24+24 drug schedule.

The drug doses used were 5 μM (A2780), 10 μM (SW1573 and HBL-100), and 15 μM (T-47D and WiDr). Control cells were incubated in the absence of test drug. The results from the control and treated human breast cancer T-47D cells are shown in Figure 6. This assay quantified the number of apoptotic cells; overall, the drug treatment significantly increased the proportion of apoptotic cells. These results demonstrate the ability of these compounds to induce apoptosis in all cell lines. A subtle difference was observed between the free hydroxyl compound **17a** and its acylated derivatives **17b–c** in the breast cancer cells (T-47D), the latter being more potent cytotoxic agents.

Currently available anticancer therapeutics are expensive, toxic, and can have limited effectiveness in treating the disease. For this reason, natural products continue to be a valuable source of novel antitumor drugs or lead compounds. In this study, we have used the 1,2-dihydroxy-4-oxo alkanols present in avocado as templates to design new drugs.

The straightforward synthesis of compounds **17a–c** and their biological activity as cell cycle arresting agents make them relevant leads for the development of novel chemotherapeutics. Our results indicate that the compounds induce permanent damage in a panel of representative human cancer cell lines. Although the exact target remains unknown, we showed that the compounds are able to induce apoptosis, even after drugs were washed away and cells were allowed to recover for a 24 h period in drug-free medium. Our new compounds show a similar effect on breast cancer cell lines as the results reported for persin (**3**).[17] Furthermore, the antiproliferative activity of compounds **17a–c** is not limited to drug-sensitive cell lines, such as A2780 and HBL-100, but also to more resistant cell lines such as T-47D and WiDr.[20]

While defects in the G_0/G_1 arrest checkpoint may enhanced cell proliferation, defects in the G_2/M arrest checkpoint cause

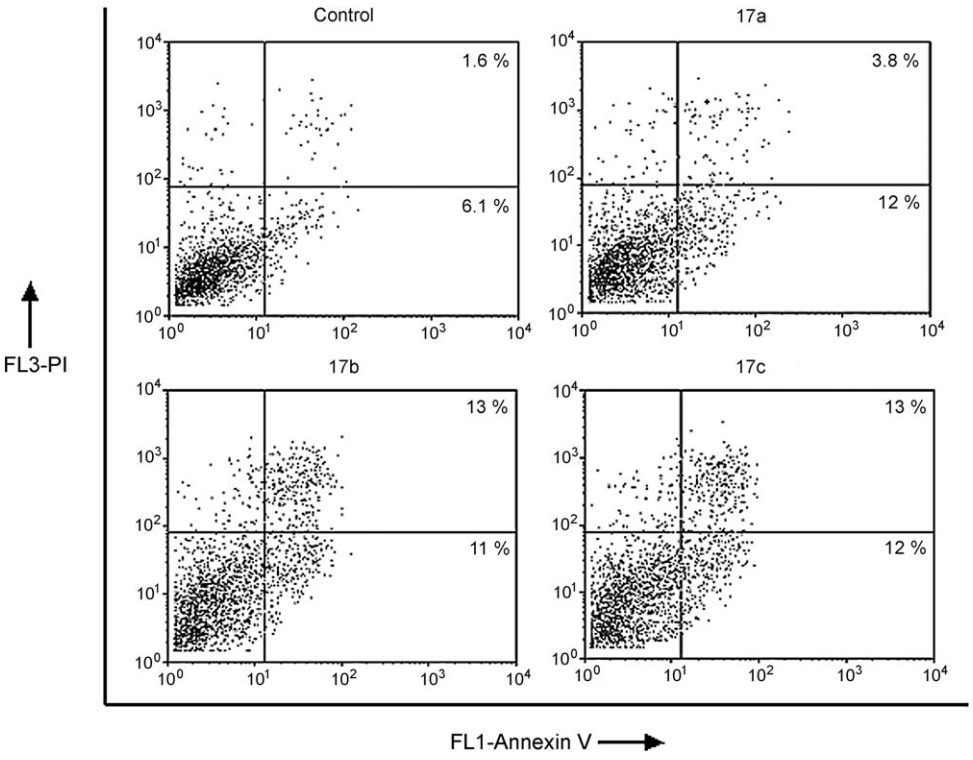

Figure 6. Annexin V and PI staining of untreated T-47D cells (Control) and T-47D cells treated for 24 h with compounds **17a–c**, followed by a 24 h drug-free period (24 + 24 drug schedule). Viable cells are Annexin− and PI−, early apoptotic cells are Annexin+ and PI−, and late apoptotic cells are Annexin+ and PI+. Quantification of apoptosis showed the percentage of cells that were apoptotic.

the cell to enter mitosis and undergo apoptosis. Induction of apoptosis is the most potent defense against cancer. Indeed, the immune system destroys cancerous cells, and most chemotherapeutic and chemopreventive agents inhibit tumor cell proliferation, by inducing apoptosis. Therefore, drugs that induce cell cycle arrest in the G_2/M phase are valuable candidates for cancer chemotherapy. In addition, the G_2/M phase of the cell cycle is the most radiosensitive phase, and this property is exploited in clinical trials combining anticancer drugs with radiation therapy.[21]

Conclusions

In conclusion, we have synthesized a series of β′-acyloxy-α,β-unsaturated ketones in a limited number of steps. These compounds show remarkable biological activity towards human cancer cell lines, including cell cycle arrest and apoptosis induction. More experiments are needed to validate the usefulness of these derivatives as potential therapeutics in combination with existing chemo- and radiotherapy, or alone. In light of the differences observed in the biological activity of compounds **17a–c**, a more detailed structure–activity relationship study may be necessary in order to establish the scope and limitations of the new pharmacophore, β′-hydroxy-α,β-unsaturated ketone, and its acylated derivatives.

Experimental Section

Chemistry

DCM and THF were distilled under N_2 from CaH_2 and Na/benzophenone, respectively, immediately prior to use. All other chemicals were of reagent grade and were used without further purification. Thin layer chromatography was carried out on aluminum sheets coated with silica gel 60F254. Plates were developed using a solution of vainillin (6 g) in AcOH (40 mL), H_2SO_4 (30 mL) and EtOH (450 mL). Flash chromatography was performed using silica gel 0.25 mm E. Merck silica gel (60F-254). IR spectra were recorded on a Bruker IFS 55 spectrometer model. ^{1}H NMR spectra were recorded at 300 MHz, ^{13}C NMR spectra were recorded at 75 MHz. The samples were dissolved in $CDCl_3$ unless otherwise noted. Elemental analyses were obtained using an EA 1108 CHNS-O FISONS--instrument.

Experimental details for the synthesis of compounds **8a–b**, **16a** and **17a**, together with their spectroscopic data, have been reported previously.[22] Additional information, including analytical and spectral characterization data for compounds **16b**, **17b**, and **17c**, UV spectrum for compounds **17a** and **17b** recorded from the stability experiment, and cell cycle phase distribution of cells treated with compounds **17a–c**, can be found in the Supporting Information.

(*E*)-1-Hexyl-3-oxo-4-undecenyl acetate (16b): Acetic anhydride (170 μL, 1.8 mmol) was added to a solution of (*E*)-11-hydroxy-heptadec-7-en-9-one (**16a**, 325 mg, 1.21 mmol) in pyridine (1.2 mL) at RT and the mixture was stirred overnight. The solvent was evaporated in vacuo and the crude was purified by flash chromatography (*n*-hexane/EtOAc, 15%) to give the acetate **16b** as an oil (218 mg, 0.70 mmol, 58% yield). ^{1}H NMR (300 MHz, $CDCl_3$, 25 °C): $\delta = 6.88$ (m, 1H), 6.08 (d, $J = 1.3$, 15.8 Hz, 1H), 5.25 (m, 1H), 2.87 (dd, $J = 6.8$, 15.5 Hz, 1H), 2.65 (dd, $J = 6.0$, 15.5 Hz, 1H), 2.22 (m, 3H), 1.99 (s, 3H), 1.57 (brs, 2H), 1.43 (brs, 2H), 1.28 (brs, 12H), 0.84 ppm (m, 7H); ^{13}C NMR (300 MHz, $CDCl_3$, 25 °C): $\delta = 197.3$ (C), 170.4 (C), 148.5 (CH), 130.3 (CH), 70.8 (CH), 44.3 (CH_2), 34.1 (CH_2), 32.6 (CH_2), 32.5 (CH_2), 31.6 (CH_2), 31.5 (CH_2), 29.0 (CH_2), 28.8 (CH_2), 28.1 (CH_2), 28.0 (CH_2), 25.1 (CH_2), 22.6 (CH_3), 14.0 ppm (CH_3); FT-IR ($CHCl_3$): $\tilde{\nu} = 2929.1$, 2858.8, 1716.4, 1462.7 cm^{-1}; elemental analysis calcd (%) for $C_{19}H_{34}O_3$ (310.47): C 73.50, H 11.04; found C 73.54, H 10.95.

(*E*)-1,5-Dicyclohexyl-3-oxo-4-pentenyl acetate (17b): Acetic anhydride (165 μL, 1.74 mmol) was added to a solution of (*E*)-1,5-dicyclohexyl-5-hydroxypent-1-en-3-one (**17a**, 308 mg, 1.17 mmol) in pyridine (1.2 mL) at RT and the mixture was stirred overnight. The solvent was evaporated in vacuo and the crude was purified by flash chromatography (*n*-hexane/EtOAc, 15%) to give acetate **17b** as an oil (187 mg, 0.61 mmol, 52% yield). ^{1}H NMR (300 MHz, $CDCl_3$, 25 °C): $\delta = 6.73$ (dd, $J = 6.8$, 16.0 Hz, 1H), 6.0 (dd, $J = 1.2$, 16.0 Hz, 1H), 5.11 (m, 1H), 2.72 (ddd, $J = 7.9$, 15.6, 23.5 Hz, 2H), 2.09 (m, 1H), 1.96 (s, 3H), 1.54 (m, 11H), 1.15 ppm (m, 10H); ^{13}C NMR (300 MHz, $CDCl_3$, 25 °C): $\delta = 197.7$ (C), 170.1 (C), 152.7 (CH), 127.6 (CH), 73.8 (CH), 41.4 (CH_2), 41.1 (CH), 40.4 (CH), 31.5 (CH_2), 28.5 (CH_2), 27.7 (CH_2), 26.0 (CH_2), 25.8 (CH_2), 25.7 (CH_2), 25.6 (CH_2), 25.4 (CH_2), 20.8 ppm (CH_3); FT-IR ($CHCl_3$): $\tilde{\nu} = 2928.0$, 2853.0, 1735.4, 1450.0, 1370.0, 1240.9, 1022.6 cm^{-1}; MS (EI) *m/z* 263 $[M-Ac]^+$; elemental analysis calcd (%) for $C_{19}H_{30}O_3$ (306.44): C 74.47, H 9.87; found C 74.48, H 10.02.

(*E*)-1,5-dicyclohexyl-3-oxo-4-pentenyl benzoate (17c): Benzoyl chloride (216 μL, 1.86 mmol) was added to a solution of (*E*)-1,5-dicyclohexyl-5-hydroxypent-1-en-3-one (**17a**, 328 mg, 1.25 mmol) in pyridine (1.2 mL) at RT and the mixture was stirred overnight. The solvent was evaporated in vacuo and the crude was purified by flash chromatography (*n*-hexane/EtOAc, 15%) to give benzoate **17c** as an oil (191 mg, 0.53 mmol, 42% yield). ^{1}H NMR (300 MHz, $CDCl_3$, 25 °C): $\delta = 7.99$ (d, $J = 7.02$ Hz, 2H) 7.51 (m, 1H), 7.39 (t, $J = 7.76$ Hz, 2H), 6.75 (dd, $J = 6.74$, 16.01 Hz, 1H), 6.04 (dd, $J = 1.0$, 15.0 Hz, 1H), 5.40 (dd, $J = 5.8$, 7.3 Hz, 1H), 2.95 (dd, $J = 7.6$, 15.1 Hz, 1H), 2.85 (dd, $J = 5.2$, 13.4 Hz, 1H), 2.05 (m, 1H), 1.70 (m, 11H), 1.14 ppm (m, 10H); ^{13}C NMR (300 MHz, $CDCl_3$, 25 °C): $\delta = 197.8$ (C), 165.6 (C), 152.9 (CH), 132.6 (CH), 130.2 (CH), 129.0 (CH), 128.0 (CH), 127.7 (CH), 74.7 (CH), 41.5 (CH_2), 41.2 (CH), 40.3 (CH), 31.4 (CH_2), 28.8 (CH_2), 27.7 (CH_2), 26.1 (CH_2), 25.8 (CH_2), 25.8 (CH_2), 25.6 (CH_2), 25.4 ppm (CH_2); FT-IR ($CHCl_3$): $\tilde{\nu} = 2927.2$, 2853.1, 1718.0, 1450.0, 1272.6, 1111.5, 711.5 cm^{-1}; MS (EI) *m/z* 263 $[M-Bz]^+$; elemental analysis: calcd (%) for $C_{24}H_{32}O_3$ (368.60): C 78.22, H 8.75; found C 78.24, H 8.87.

Stability test for compound 17b: In order to test the stability of compound **17b** under physiological pH, the following experimental procedure was run on a UV Transparent Greiner 96-well plate (Sigma, St Louis, MO). Phosphate buffered saline (PBS) solution (200 μL) (Sigma, St. Louis, MO) was added to each experimental well. The wells were treated with compound **17a** or **17b** in DMSO (1 μL, 0.04 M), DMSO alone (1 μL) was added to the control wells. The plate was warmed to 37 °C and kept at this temperature until the end of the experiment. Each sample was tested in quintuplicate. The UV spectrum of each cell was recorded in the wavelength range 200–300 nm at the experimental time intervals 0, 24 and 48 h of incubation.

Biology

All starting materials were commercially available research-grade chemicals and used without further purification. RPMI 1640

medium was purchased from Flow Laboratories (Irvine, UK), fetal calf serum (FCS) was from Gibco (Grand Island, NY), trichloroacetic acid (TCA) and glutamine were from Merck (Darmstadt, Germany), and penicillin G, streptomycin, DMSO and sulforhodamine B (SRB) were from Sigma (St Louis, MO).

Cells, culture and plating: The human solid tumor cell lines A2780 and SW1573 were used in this study. Cells were maintained in 25 cm^2 culture flasks in RPMI 1640 supplemented with 5% heat inactivated fetal calf serum and 2 mM L-glutamine in a 37 °C, 5% CO_2, 95% humidified air incubator. Exponentially growing cells were trypsinized and re-suspended in antibiotic containing medium (100 units penicillin G and 0.1 mg of streptomycin per mL). Single cell suspensions displaying > 97% viability by trypan blue dye exclusion were subsequently counted. After counting, dilutions were made to give the appropriate cell densities for inoculation onto 96-well microtiter plates. Cells were inoculated in a volume of 100 μL per well at densities of 7000 (A2780), 6000 (SW1573 and HBL-100) and 15 000 (WiDr and T-47D) cells per well, based on their doubling times.

Chemosensitivity testing: Chemosensitivity tests were performed using the SRB assay of the NCI with slight modifications.[9] Briefly, compounds were initially dissolved in DMSO at 400 times the desired final maximum test concentration. Control cells were exposed to an equivalent concentration of DMSO (0.25% *v/v*, negative control). Each agent was tested in triplicate at different dilutions in the range of 1–100 μM. The drug treatment was started on day 1 after plating. Drug incubation times were 48 h, after which time cells were precipitated with 25 μL ice-cold TCA (50% *w/v*) and fixed for 60 min at 4 °C. Then the SRB assay was performed. The optical density (OD) of each well was measured at 492 nm, using BioTek's PowerWave XS Absorbance Microplate Reader. Values were corrected for background OD from wells only containing medium. The percentage growth (PG) was calculated with respect to untreated control cells (C) at each of the drug concentration levels based on the difference in OD at the start (T_0) and end of drug exposure (T), according to NCI formulas. Therefore, if T is greater than or equal to T_0 the calculation is $100\times[(T<M->T_0)/(C<M->T_0)]$. If T is less than T_0 denoting cell killing the calculation is $100\times[(T<M->T_0)/(T_0)]$. The effect is defined as percentage of growth, where 50% growth inhibition (GI_{50}), total growth inhibition (TGI), and 50% cell killing (LC_{50}) represent the concentration at which PG is +50, 0, and −50, respectively. With these calculations a PG value of 0 corresponds to the number of cells present at the start of drug exposure, while negative PG values denote net cell kill.

Cell cycle analysis: Cells were seeded in a six well plates at a density of $0.7–1\times10^6$ cells/well. After 24 h the products were added to the respective well and incubated for an additional period of 24 h. Cells were trypsinized, harvested, transferred to test tubes (12× 75 mm) and centrifuged at 1500 rpm for 10 min. The supernatant was discarded and the cell pellets were re-suspended in 200 μL of cold PBS and fixed by the addition of 3 mL ice-cold 70% EtOH. Fixed cells were incubated overnight at −20 °C after which time were centrifuged at 1500 rpm for 10 min. The cell pellets were re-suspended in 500 μL PBS. Then, 20 μL of DNAse-free RNAse (200 μL mL^{-1}) and 10 μL of PI (40 μL mL^{-1}) were sequentially added. The mixture was incubated in the dark at 37 °C for 30 min. Flow cytometric determination of DNA content (25 000 cells/sample) was analyzed on a FACS Calibur Flow Cytometer (Becton Dickinson, San José, CA, USA). The fractions of the cells in G_0/G_1, S, and G_2/M phase were analyzed using cell cycle analysis software, ModFit LT 3.0 (Verity Software House, Topsham, ME, USA).

Annexin V binding: Cells were seeded in six well plates at a density of $0.25–0.5\times10^6$ cells. After 24 h, the test drug was added and the cells incubated for period of 24 h. Then, the medium was removed with suction and substituted by drug-free fresh medium. Cells were incubated for an additional period of 24 h. Then, cells were trypsinized, harvested, transferred to test tubes (12×75 mm) and centrifuged at 400 g for 10 min. The supernatant was discarded and the cells pellets were re-suspended in 100 μL of ice-cold 1× Binding Buffer (0.1 M Hepes/NaOH (pH = 7.4) 1.4 M NaCl, 25 mM $CaCl_2$).

Annexin staining protocol was performed according to the manufacturer's protocol (Annexin V-FITC apoptosis detection Kit I, Becton Dickinson, San José, CA), with minor modifications. Cells were stained by the addition of both 5 μL Annexin V-FITC and 5 μL PI solution. Samples were gently vortexed and incubated for 15 min at RT in the dark. Then, 400 μL of 1x binding buffer was added to each tube. The samples were analyzed by flow cytometry using Cell Quest Pro software (Becton Dickinson, San José.CA). Typically, 10, 000 events were collected using excitation/emission wavelengths of 488/525 and 488/675 nm for Annexin V and PI, respectively. Results were processed using WinMDI 2.8 free software.

Acknowledgements

This research was supported by the Spanish MEC, co-financed by the European Regional Development Fund (CTQ2005-09074-C02-01/BQU), the Canary Islands Government, the Spanish MSC-ISCIII FIS (RD06/0020/1046), and the Fundación Canaria de Investigación y Salud (PI 1/06 and PI 35/06). L.G.L. thanks the Spanish MSC-FIS for a postdoctoral contract. R.M.C. thanks the Spanish MEC for a postgraduate FPU grant. M.C.V.-H. thanks the Spanish MSC for a postdoctoral CIBERER U740 contract. P.O.M. thanks the Spanish MEC for a FPI postgraduate grant. J.I.P. and J.M.P. thank the Spanish MEC-FSE for a Ramón y Cajal contract.

Keywords: structure–activity relationships · antitumor agents · apoptosis · cell cycle · iron(III) chloride

[1] a) L. Costantino, D. Barlocco, *Curr. Med. Chem.* **2006**, *13*, 65–85; b) R. W. DeSimone, K. S. Currie, S. A. Mitchell, J. W. Darrow, D. A. Pippin, *Comb. Chem. High Throughput Screening* **2004**, *7*, 473–494.
[2] B. B. Aggarwal, S. Shishodia, *Biochem. Pharmacol.* **2006**, *71*, 1397–1421.
[3] H. Ding, Y.-W. Chin, A. D. Kinghorn, S. M. D'Ambrosio, *Semin. Cancer Biol.* **2007**, *17*, 386–394.
[4] N. H. Oberlies , L. L. Rogers, J. M. Martin, J. L. McLaughlin, *J. Nat. Prod.* **1998**, *61*, 781–785.
[5] O. K. Kim, A. Murakami, D. Takahashi, Y. Nakamura, H. W. Kim, H. Ohigashi, *Biosci. Biotechnol. Biochem.* **2000**, *64*, 2500–2503.
[6] J. M. Padrón, P. O. Miranda, J. I. Padrón, V. S. Martín, *Bioorg. Med. Chem. Lett.* **2006**, *16*, 2266–2269.
[7] P. O. Miranda, M. A. Ramírez, J. I. Padrón, V. S. Martín, *Tetrahedron Lett.* **2006**, *47*, 283–286.
[8] D. Tejedor, D. González-Cruz, A. Santos-Expósito, J. J. Marrero-Tellado, P. de Armas, F. García-Tellado, *Chem. Eur. J.* **2005**, *11*, 3502–3510, and references therein.
[9] P. O. Miranda, J. M. Padrón, J. I. Padrón, J. Villar, V. S. Martín, *ChemMedChem* **2006**, *1*, 323–329.
[10] a) D. D. Díaz, P. O. Miranda, J. I. Padrón, V. S. Martín, *Curr. Org. Chem.* **2006**, *10*, 457–476; b) C. Bolm, J. Legros, J. Le Paih, *Chem. Rev.* **2004**, *104*, 6217–6264.
[11] For a definition of this terminology, see: D. Tejedor, A. Santos-Expósito, F. García-Tellado, *Chem. Commun.* **2006**, 2667–2669.

[12] The NCI renamed the IC_{50} value, the concentration that causes 50% growth inhibition, the GI_{50} value so as to emphasize the correction for the cell count at time zero. A. Monks, D. A. Scudiero, P. Skehan, R. H. Shoemaker, K. D. Paull, D. T. Vistica, C. Hose, J. Langley, P. Cronice, M. Vaigro-Wolf, M. Gray-Goodrich, H. Campbell, M. R. Mayo, *J. Natl. Cancer Inst.* **1991**, *83*, 757–766.
[13] C. A. Lipinski, F. Lombardo, B. W. Dominy, P. J. Feeney, *Adv. Drug Delivery Rev.* **2001**, *46*, 3–26.
[14] Software-predicted lipophilicity of the compounds was calculated with the program Clog *P*, accessible from www.daylight.com/daycgi/clogp, working with Hansch-Leo's "fragment constant" method.
[15] A. W. Murray, *Cell* **2004**, *116*, 221–234.
[16] J. M. Padrón, G. J. Peters, *Invest. New Drugs* **2006**, *24*, 195–202.
[17] A. J. Butt, C. G. Roberts, A. A. Seawright, P. B. Oelrichs, J. K. MacLeod, T. Y. E. Liaw, M. Kavallaris, T. J. Somers-Edgar, G. M. Lehrbach, C. K. Watts, R. L. Sutherland, *Mol. Cancer Ther.* **2006**, *5*, 2300–2309.
[18] C. G. Roberts, E. Gurisik, T. J. Biden, R. L. Sutherland, A. J. Butt, *Clin. Chim. Acta* **2002**, *326*, 27–45.
[19] a) F. L. Kiechle, X. Zhang, *Mol. Cancer Ther.* **2007**, *6*, 2777–2785; b) A. L. Edinger, C. B. Thompson, *Curr. Opin. Cell. Biol.* **2004**, *16*, 663–669.
[20] P. E. Pizao, G. J. Peters, J. van Ark-Otte, L. A. Smets, E. Smitskamp-Wilms, B. Winograd, H. M. Pinedo, G. Giaccone, *Eur. J. Cancer* **1993**, *29 A*, 1566–1573.
[21] H. Choy, *Crit. Rev. Oncol. Hematol.* **2001**, *37*, 237–247.
[22] P. O. Miranda, D. D. Díaz, J. I. Padrón, M. A. Ramírez, V. S. Martín, *J. Org. Chem.* **2005**, *70*, 57–62.

Received: July 8, 2008
Published online on October 9, 2008

